Cell Transplantation, Vol. 24, pp. 2423–2433, 2015
Printed in the USA.

0963-6897/15 $90.00 + .00
DOI: http://dx.doi.org/10.3727/096368915X687480
E-ISSN 1555-3892
www.cognizantcommunication.com

Human Bone Marrow Stromal Cells Differentiate Into Corneal Tissue and Prevent Ocular Graft-Versus-Host Disease in Mice

Luis Ignacio Sánchez-Abarca,*†# Emiliano Hernández-Galilea,‡# Rebeca Lorenzo,‡# Carmen Herrero,†# Almudena Velasco,§# Soraya Carrancio,† Teresa Caballero-Velázquez,*† José Ignacio Rodríguez-Barbosa,¶ Marta Parrilla,§ Consuelo Del Cañizo,†# Jesús San Miguel,** José Aijón,§# and José Antonio Pérez-Simón*†

*Department of Hematology, University Hospital Virgen del Rocío/IBIS/CSIC/University of Seville, Seville, Spain
†Department of Hematology, University Hospital of Salamanca, Salamanca, Spain
‡Department of Surgery, Ophthalmology Service, University Hospital of Salamanca, University of Salamanca, Salamanca, Spain
§Department Cell Biology and Pathology, INCyL, University of Salamanca, Salamanca, Spain
¶Immunobiology Section, Institute of Biomedicine, University of León, León, Spain
#Institute of Biomedicine Investigation of Salamanca (IBSAL), Salamanca, Spain
**Clinica Universidad de Navarra, Centro de Investigación Médica Aplicada (CIMA), Pamplona, Spain

Clinical trials have assessed the use of human bone marrow stromal cells (hBMSCs) for the treatment of immune-related disorders such as graft-versus-host disease (GVHD). In the current study, we show that GFP^+-transduced hBMSCs generated from bone marrow migrate and differentiate into corneal tissue after subconjunctival injection in mice. Interestingly, these hBMSCs display morphological features of epithelial, stromal, and endothelial cells and appear at different layers and with different morphologies depending on their position within the epithelium. Furthermore, these cells display ultrastructural properties, such as bundles of intermediate filaments, interdigitations, and desmosomes with GFP^- cells, which confirms their differentiation into corneal tissues. GFP^+-transduced hBMSCs were injected at different time points into the right eye of lethally irradiated mice undergoing bone marrow transplantation, which developed ocular GVHD (oGVHD). Remarkably, hBMSCs massively migrate to corneal tissues after subconjunctival injection. Both macroscopic and histopathological examination showed minimal or no evidence of GVHD in the right eye, while the left eye, where no hBMSCs were injected, displayed features of GVHD. Thus, in the current study, we confirm that hBMSCs may induce their therapeutic effect at least in part by differentiation and regeneration of damaged tissues in the host. Our results provide experimental evidence that hBMSCs represent a potential cellular therapy to attenuate oGVHD.

Key words: Human bone marrow stromal cells (hBMSCs); Ocular graft-versus-host disease (oGVHD); Cornea; Subconjunctival injection; Cell migration; Differentiation

INTRODUCTION

Human bone marrow stromal cells (hBMSCs) are non-hematopoietic stromal cells capable of differentiating into, and contributing to, the regeneration of mesenchymal tissues (8). More recently, it has been shown that hBMSCs, under certain experimental conditions, can also differentiate into cell types with features of endodermal and neuroectodermal cell lineages (10,22,36). Intravenously infused hBMSCs migrate to a variety of organs and integrate into tissues, with preferential location in injured tissues (10,22). Human bone marrow-derived stromal cells expand in vitro, and their progeny retain the abilities to differentiate into several cell lineages and to suppress the immune response (36). Thus, it is possible to produce enough stromal cells from a limited number of cells obtained following bone marrow (BM) harvest. Based on these properties, human mesenchymal stromal cells (hMSCs) are ideal candidates for tissue engineering, and several therapeutic applications are currently being evaluated. In this regard, cultured hMSCs have already been

Received July 22, 2014; final acceptance February 6, 2015. Online prepub date: February 18, 2015.
Address correspondence to José Antonio Pérez-Simón, M.D., Ph.D., Servicio de Hematología, Instituto de Biomedicina de Sevilla (IBIS)/ Hospital Universitario Virgen del Rocío/CSIC/Universidad de Sevilla, Avenida de Manuel Siurot s/n, 41013 Sevilla, Spain. Tel: +34-955-013260; Fax: +34-955-013265; E-mail: josea.perez.simon.sspa@juntadeandalucia.es *or* Emiliano Hernández-Galilea, M.D., Servicio de Oftalmología, Hospital Universitario de Salamanca, Paseo de San Vicente s/n 37007 Salamanca, Spain. Tel: +34-629838631; Fax: +34-923291113; E-mail: egalilea@usal.es

infused into human subjects for the treatment of diseases such as graft-versus-host disease (GVHD), with promising results (33,36). It is still a matter of debate whether these therapeutic benefits are due to engraftment and local transdifferentiation into injured tissues, or just the consequence of a paracrine effect. In this regard, Devine et al. described that ex vivo expanded hMSCs were found in different tissues several months following infusion in nonhuman primates (10). By contrast, Chapel et al. showed that the beneficial effect observed after the injection of hMSCs is not related to transdifferentiation but to a paracrine effect, which modulates other cell lineages' function (9). Thus, while the original perception was that hMSCs contribute to tissue regeneration, more recent data suggest that the main mechanism of hMSC function is through the release of soluble mediators that elicit the observed biological response (21). Furthermore, several studies have been reported describing that hMSCs only transiently persist after systemic infusion in the host (20).

Normal corneal tissue is located in the anterior segment of the eye. It is comprised of three main layers: epithelium, stroma, and endothelium. Approximately 90% of the corneal volume is stroma, a collagenous mesenchymal tissue composed of multiple lamellae of parallel collagen fibrils (34). It has recently been shown that bone marrow-derived cells are normal components of human corneal stroma, even in the absence of inflammation (13). The corneal epithelium is a self-renewing tissue maintained by limbal epithelial stem cells (7,34,35).

From an immunological point of view, the normal avascular cornea has been considered as an immune-privileged site, without functional antigen-presenting cells (APCs) and largely devoid of BM-derived cells. However, this notion has been challenged by the evidence of the presence of large numbers of resident BM-derived cells, in both the epithelium and stroma of the normal cornea (2,17,18). These infiltrating cells are likely targeting the eye after allogeneic stem cell transplantation. In this regard, increasing evidence suggests that donor T cells may induce tissue damage into the cornea, as previously shown by our group in an animal model of oGVHD, which involves epithelium, endothelium, and limbus (27).

With this background, and considering that the immunomodulatory effect of hMSCs and their potential capability to regenerate damaged tissues could be useful in the clinical setting, in the current study we attempted to investigate the distribution of hBMSCs in the cornea after a subconjunctival injection both in control mice and after bone marrow transplantation (BMT). Interestingly, we found that hBMSCs migrate to the cornea and differentiate into corneal epithelium, stroma, and endothelium. This migration was strikingly more evident in mice with oGVHD. Furthermore, hBMSCs allowed preserving corneal integrity, thus avoiding GVHD-mediated tissue damage.

MATERIALS AND METHODS

Animals

All animal protocols were approved by the University of Salamanca Animal Care and Use Committee. Female BALB/c ($H2^d$) and male C57BL/6 ($H2^b$) mice were purchased from Charles River Laboratory, France. Animals were kept in specific pathogen-free conditions. The animals used in the facilities associated with the Experimentation Service of the University of Salamanca are kept following both the national (RD 1201/2005) and European (609/CEE) corresponding legislation regarding the protection of animals used for experimentation and other scientific aims. As well, all projects using animals are evaluated by the Animal Ethical Committee of the University of Salamanca before the commencing of the experimentation in the centers associated with the Experimentation Service (number of permission from the ethical committee JLR/bb).

Eight- to 12-week-old mice weighing 20–25 g were housed with free access to food and water ad libitum.

Two experimental groups were established:

Group I: Nontransplanted immune-competent BALB/c ($H2^d$) mice ($n = 20$), which received a subconjunctival injection of hBMSCs in the right eye and were sacrificed at different time points after injection (10, 20, 30, and 40 days).

Group II: BALB/c ($H2^d$) mice ($n = 16$), which received a subconjunctival injection of hBMSCs in the right eye on day 15 after BMT from C57BL/6 mice to generate GVHD. These BALB/c mice were sacrificed at different time points after injection (10 and 20 days).

For this purpose, donor mice C57BL/6 were sacrificed by cervical dislocation, and BM and spleen were harvested by standard techniques. Spleen cell preparations were obtained by gently crushing the tissues to release the cells. Preparations were filtered to remove debris and washed twice in phosphate-buffered saline (PBS; Gibco, Invitrogen, Paisley, UK) for injection. Recipient BALB/c ($H2^d$) mice received total body irradiation (850 cGy divided in two fractions of 2.06 min) from a Cs source (GammaCell 200; Nordion International, Ottawa, ON, Canada). Irradiation was followed by the intravenous infusion of 5×10^6 C57BL/6 allogeneic donor BM cells with splenocytes (5×10^6 cells intravenously) as a source of allogeneic T cells. The degree of systemic GVHD was assessed by a standard scoring system that incorporates five clinical parameters: weight loss, posture (hunching), activity, fur texture, and skin integrity. Each parameter received a score ranging from 0 (minimum) to 2 (maximum) (6). Immune-competent and transplanted mice were ear punched, and individual weights were obtained and recorded on day 0 and twice a week thereafter. All moribund mice were humanely sacrificed.

In order to evaluate oGVHD, three clinical features were monitored, as previously reported: periocular fur, eyelid margin, and blepharospasm. Each sign was scored with 0 (no loss of periocular fur, no crusting of the eyelid margin/erythematous lids, no blepharospasm), 1 (one feature of the following: loss of periocular fur, crusting of the eyelid margin/erythematous lids, blepharospasm), and 2 (two or three of the previously mentioned features) (27). Macroscopic and histological examinations of the enucleated eyes were performed. All experiments were performed at least twice and included a minimum of four animals per group.

Subconjunctival Injection of hBMSCs

Mice were anesthetized with 4.0% isoflurane (Abbott Laboratories, UK) in air for 2 min and maintained with 1.5% isoflurane. We administered a 20-µl subconjunctival injection of physiological saline (B. Braun Medical Inc., Irvine, CA, USA) containing 2×10^5 hBMSCs at 1–2 mm of the right eye sclerocorneal limbus with a 27-gauge Terumo Myjector (Terumo Europe, Leuven, Belgium). The injection was performed 5 min after the start of induction of anesthesia. Ciprofloxacin drops (Alcon Cusi S.A., Alcobendas, Spain) were administered before hBMSCs were injected, and povidone-iodine 0.5% (Meda Pharma S.A.U., Spain) was instilled after injection, to avoid infections. Mice received the subconjunctival injection on day 15 after transplantation and were euthanized at different time points after injection. Afterward, we removed the right and left eyes. The left eye was used as control.

Chimerism by Flow Cytometry

Hematopoietic cell chimerism was monitored in peripheral blood, spleen, and bone marrow 14 days after transplantation. By that time 100% chimerism was from donor origin in all organs analyzed (data not shown). For this purpose, 5×10^5 cells suspended in PBS were stained by direct immunofluorescence using monoclonal antibodies (mAbs) conjugated with the following fluorochromes: fluorescein isothiocyanate (FITC); phycoerythrin (PE); peridin chlorophyll protein-Cyanin 5.5 (PerCP-Cy5.5), and Alexa Fluor 647. Specific antibodies were purchased from Becton Dickinson Bioscience Pharmingen (San Jose, CA, USA). The following combination was used: 10 µl of anti-H-2D^b-FITC/5 µl of anti-H-2D^d-PE/10 µl of anti-CD45-PerCP-Cy5.5/3 µl of anti-CD34-Alexa Fluor or 10 µl of anti-H2D^b-FITC/5 µl of anti-H2D^d-PE/10 µl of anti-CD45-PerCP-Cy5.5/3 µl of anti-CD3-Alexa Fluor. The final volume (resuspended cells, mAbs and PBS) was 100 µl. Data were acquired immediately after the staining was completed, using a FACSCalibur flow cytometer equipped with the CellQuest™ program (Becton Dickinson). Data were analyzed using the Infinicyt program (Cytognos, Salamanca, Spain).

hBMSCs Culture and Staining

hBMSCs were isolated from BM cells of five healthy volunteer donors (three males/two females) with a median age of 40 years (range 28–52 years) after informed consent had been obtained, in accordance with the local Ethics Committee. Ten milliliters of BM were taken by iliac crest aspiration under local anesthesia, following standard institutional procedures. Mononuclear cells (MNCs) were isolated by Ficoll-Paque density-gradient centrifugation (GE Healthcare Bio-Sciences, Uppsala, Sweden) and cultured in standard culture medium (Dulbecco's modified Eagle's medium-low glucose (DMEM; Gibco) supplemented with 10% fetal calf serum (FCS; BioWhittaker, Lonza, Verviers, Belgium) and 1% penicillin/streptomycin; Gibco) as described previously (5). Cells were seeded at an initial density of 1×10^6 cells/cm^2 and incubated in a humidified atmosphere with 5% CO_2. hBMSCs were expanded in T75 culture flasks (Corning, Corning, NY, USA) and cultured as previously described (37). After the third passage, hBMSCs were assessed following the minimal criteria recommended by the International Society for Cellular Therapy (ISCT) (11). Differentiation capacity to osteoblasts, adipocytes, and chondrocytes was done using NH Osteodiff, NH Adipodiff, and NH Chondrodiff medium, respectively (all from Miltenyi Biotec, Bergisch Gladbach, Germany) (4). For immunophenotypic analysis, 5×10^5 cells suspended in PBS were stained by direct immunofluorescence using mAbs. hBMSCs were incubated for 15 min with 5 µl of FITC-conjugated CD90, 10 µl of FITC-conjugated CD44, 10 µl of FITC-conjugated CD34, 10 µl of PE-conjugated CD73, 10 µl of PE-conjugated CD14, 10 µl of PE-conjugated CD166, 10 µl of PerCP-conjugated anti-HLA-DR, 10 µl of PerCP-Cy5.5-conjugated CD45, and 10 µl of PerCP-Cy5.5-conjugated CD19 (all from Becton Dickinson), and 5 µl of allophycocyanine (APC)-conjugated CD105 (R&D Systems, Minneapolis, MN, USA). The final volume (resuspended cells, mAbs, and PBS) was 100 µl. Data were acquired immediately after the staining was completed, using a FACSCalibur flow cytometer equipped with the CellQuest™ program (Becton Dickinson). Data were analyzed using the Infinicyt program (Cytognos).

Lentiviral Vector Production and hBMSC Transduction

For virus production, 2×10^6 human embryonic kidney (HEK; American Type Culture Collection, Manassas, VA, USA) 293T cells were seeded on 15-cm-diameter culture dishes (Becton Dickinson) 1 day before transfection and cultured in standard conditions, at 37°C in 5% CO_2 and maintained in DMEM (Gibco), supplemented with 10% FCS (BioWhittaker) and penicillin (100 U/ml), streptomycin (0.1 mg/ml) (Gibco). Briefly, 293T cells were transfected with the envelope vector pLV-VSVG,

the packaging vector psPax2 (the vectors were kindly provided by Dr. Anton Martens Netherlands), and the LV vector containing the green fluorescence protein (GFP) gen pWPI (Addgene plasmid 12254) by using the calcium phosphate DNA precipitation method, following the previously described method (16). The medium containing lentiviral supernatant was collected 48 h after transfection, filtered through a 0.45-mm pore filter (BD Falcon, manufactured for Corning Incorporated, Durham, NC, USA), pooled, and stored at −80°C until use. The titer of the virus supernatant was estimated by transducing 293T cells with different dilutions, and the transduction efficiency and the frequency of transduced GFP hBMSCs was determined by flow cytometry. Titer was calculated using the following formula: (cell concentration at the day of transduction)×(virus supernatant dilution)×(% GFP^+ cells)/total volume.

Passage two hBMSCs were transduced when they reached 50% confluence. Transductions were carried out in the presence of 8 μg/ml hexadimethrine bromide (polybrene; Sigma-Aldrich, Steinheim, Germany) and 1:8 diluted lentiviral supernatants from 293T lentiviral packaging cells. Twenty-four hours later, the transduction medium was replaced with fresh medium. At 90% confluence, cells were harvested, and GFP^+ cells were analyzed by flow cytometry to determine transduction efficiency.

Immunohistochemistry

The enucleated eyes were fixed in 4% paraformaldehyde (Carlo Erba Reagents, Val-de-Reuil, France) in phosphate buffer 0.1 M, pH 7.4 (PBS), for 12 h at 4°C. After several washes in PBS, eyes were cryoprotected in 50% sucrose (Panreac Química S.A.U., Barcelona, Spain), embedded in OCT (Sakura Finetek Europe B.V. Zoeterwoude, NL), and cut in 12-μm sections on a Cryostat Leica CM 2000 (Leica Microsystems, Nussloch, Germany). Several sections were stained with hematoxylin and eosin for structural control.

After hydrating the sections in PBS 0.1 M, pH 7.4, with 0.02% Triton X-100 (PBS-TX; Sigma-Aldrich), sections were blocked with 2% normal goat (Sigma-Aldrich) or donkey serum (Jackson ImmunoResearch Europe Ltd., Suffolk, UK), depending on the source of the antibody used, in PBS-TX for 2 h at room temperature (RT). After that, sections were incubated overnight at RT with the primary antibodies (Table 1) diluted in the blocking mixture. After washing in PBS, sections were incubated in 1:250 secondary antibodies conjugated with Cy2, A488, and Cy3 fluorescent dyes (Jackson). After the final washes, 1 μg/ml 4,6-diamidine-2-phenyl indole, dihydrochloride (DAPI; Sigma-Aldrich) in PBS was added. Sections were mounted with an antifading mixture (Fluoromount™ Aqueous Mounting Medium; Sigma-Aldrich) (31).

For histological analysis, hematoxylin (Sigma-Aldrich International, Switzerland) and eosin (Panreac Química, Spain) staining was performed.

Immunogold Labeling and Imaging

The corneas were dissected out and fixed in 4% paraformaldehyde and 0.2% glutaraldehyde (Sigma-Aldrich) in PBS for 12 h at 4°C. After several washes in PBS, corneas were cryoprotected in 25% sucrose and 10% glycerol (Merck KGaA, Darmstadt, Germany) in PBS, frozen and thawed three times, and washed with PBS. The immunogold labeling protocol was performed as described by Parrilla et al. (31). The goat polyclonal anti-GFP antibody concentration used is indicated in Table 1 and the ultrasmall gold-conjugated donkey anti-goat secondary antibody (Aurion, NL) was diluted 1:100. After that, the corneas were fixed with 0.5% osmium tetroxide (Electron Microscopy Sciences, Hatfield, PA, USA) for 20 min, at RT, dehydrated at 4°C, and flat embedded in Epon 12 resin (EMS). Ultrathin sections were stained with 2% aqueous uranyl acetate (Merck KGaA) and lead citrate (Merck KGaA).

Rabbit anti-MIF antibody (macrophage migration inhibitory factor) reacts specifically against ocular MIF protein in mouse cells (28,30,38). MIF staining was performed in order to ascertain whether the images obtained were the result of the fusion of GFP^+ hMCSs with epithelial, endothelial, or stromal cells from mice, or due to a true differentiation of hMCSs into epithelium, endothelium, or keratocytes. Thus, GFP^+/MIF^- cells are of human origin using this approach. Similarly, specific anti-human mitochondrial staining was also performed in order to identify human cells as $mitochondria^+/MIF^-$.

Some of the light microscopy images were obtained with an Olympus Apogee digital camera coupled to an Olympus AX-70 photomicroscope, and the rest of the fluorescent images were obtained with a laser scanning spectral confocal microscope (Leica TCS SP2). The ultrathin sections were observed in a Zeiss EM900 electron microscope, and the pictures were taken with the coupled digital camera using ImageSP software (SYS-PRO, Minsk, Belarus). Original pictures were further processed with Adobe Photoshop CS4 software.

Western Blot Analysis

The corneas, retinas, remaining ocular tissues, brain, and cultured hBMSCs were separately homogenized mechanically in 200 μl of RIPA buffer (Santa Cruz Biotech). After that, the protein concentration of each sample was measured with a nanophotometer (Implen). Fifty micrograms of each sample was boiled in sample buffer [2% sodium dodecyl sulfate (SDS); Sigma-Aldrich], 10% glycerol, 700 mM β-mercaptoethanol (Sigma-Aldrich),

62.5 mM Tris-HCl (pH 6.8; Sigma-Aldrich), 0.05% bromophenol blue (Sigma-Aldrich), chilled in ice and loaded on 10–12% SDS-polyacrylamide gel (Amresco, OH, USA) under reducing conditions. After electrophoresis, proteins were transferred to nitrocellulose membranes (Macherey-Nagel, Düren, Germany), blocked, and immunolabeled with antibodies (Table 1) diluted in 1% bovine serum albumin (BSA; Sigma-Aldrich), 0.1% Tween20 in TBS (50 mM Tris-HCl, pH 8, 150 mM NaCl) overnight at 4°C. After washes with TBS, the membranes were incubated with 1:5,000 anti-goat/anti-rabbit (Sigma-Aldrich) or 1:30,000 anti-mouse (Sigma-Aldrich), conjugated with alkaline phosphatase for 1 h at RT. The staining was obtained with NBT (nitro-blue-tetrazolium; Roche Applied Science) and BCIP (5-bromo-4-chloro-3-indolyl-phosphate; Roche Applied Science).

RESULTS

Group I: hBMSCs Migrate and Differentiate Into Corneal Cells

We first used the Western blot (WB) assay to test the specificity of the anti-GFP antibody (AB5450; Abcam) and the anti-human mitochondria (MAB1273; Millipore) for the detection of GFP and mitochondria located in transduced hBMSCs. This study demonstrated a single band of 27 kDa corresponding to the estimated molecular weight for GFP protein (Accession# P42212, NCBI database) and a single band of 65 kDa corresponding to the molecular weight of the epitope located in the intact mitochondria (Millipore), both exclusively located in the total protein extract of the hBMSCs. By contrast, the immunoblotting reaction was negative in cell extracts harvested from the mice's cornea, retina, and the rest of ocular tissues (eyes without retina) and brain. We also confirmed by WB analysis that MIF protein (macrophage migration inhibitory factor) was exclusively located in mouse cells. Thus, the WB results showed a single band of 12.5 kDa corresponding to the MIF protein (Accession# P34884, NCBI database) in all mouse tissues analyzed, while we did not detect any labeled band corresponding to the hBMSCs (Fig. 1). These assays were performed in order to ascertain whether the images obtained could be the result of the fusion of GFP^+ hMSCs with stromal, epithelial, or endothelial cells from mice or to a truly differentiation of hMSCs into epithelium, endothelium, or keratocytes. Thus, GFP^+/MIF^- cells are of human origin using this approach. Similarly, specific anti-human mitochondrial staining also allowed identifying human cells as $mitochondria^+/MIF^-$.

Within the group of immune-competent BALB/c mice, the right eye of the animals was treated with a subconjunctival injection of hBMSC, whereas the left eye of the same animals remained untreated. Ten days after the hBMSC injection, in the right eyes of the animals, we found $mitochondria^+$ cells with elongated morphology in the stroma and with polygonal morphology in the corneal epithelium (Fig. 2A–C). In the transition zone between conjunctiva and cornea, GFP^+ cells were seen both in the conjunctiva and cornea sides as well as in the epithelium. However, we did not find any GFP^+ cells nor in the epithelium, stroma, or endothelium layers (data not shown) of the left eyes. Thus, after 10 days of injection, subconjunctivally implanted hBMSCs were able to migrate into the three the layers of the cornea.

After 20 and 30 days post-subconjunctival injection, the number of $mitochondria^+/MIF^-$ in the cornea increased in the immune-competent mice. The main finding at these time points was that, particularly in the epithelium, hBMSCs also appeared at different layers and in morphologies varying from cubic to flattened, depending on their position. Thus, hBMSCs did integrate within the rest of the epithelium and in the stroma (Fig. 2D–O). Furthermore, at the electron microscopical level, the GFP^+ hBMSCs showed ultrastructural features typical of epithelial cells, such as bundles of intermediate filaments and interdigitations and desmosomes with other cells. In the basal stratum, we observed GFP^+ cells with cubic morphology, displaying hemidesmosomes on their basal side and desmosomes on their lateral sides

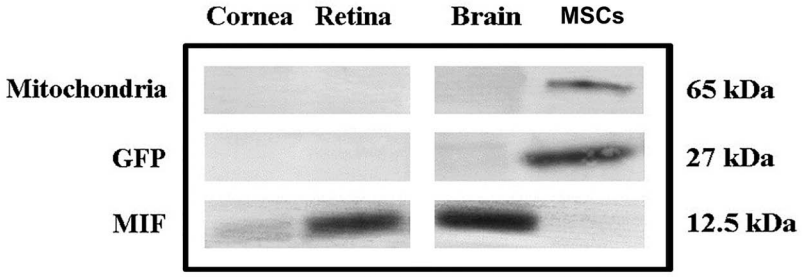

Figure 1. Western blot assays. GFP protein band (27 kDa) and intact surface mitochondria protein band (65 kDa) in hBMSCs. MIF protein band (12.5 kDa) in mice cornea, retina, and brain.

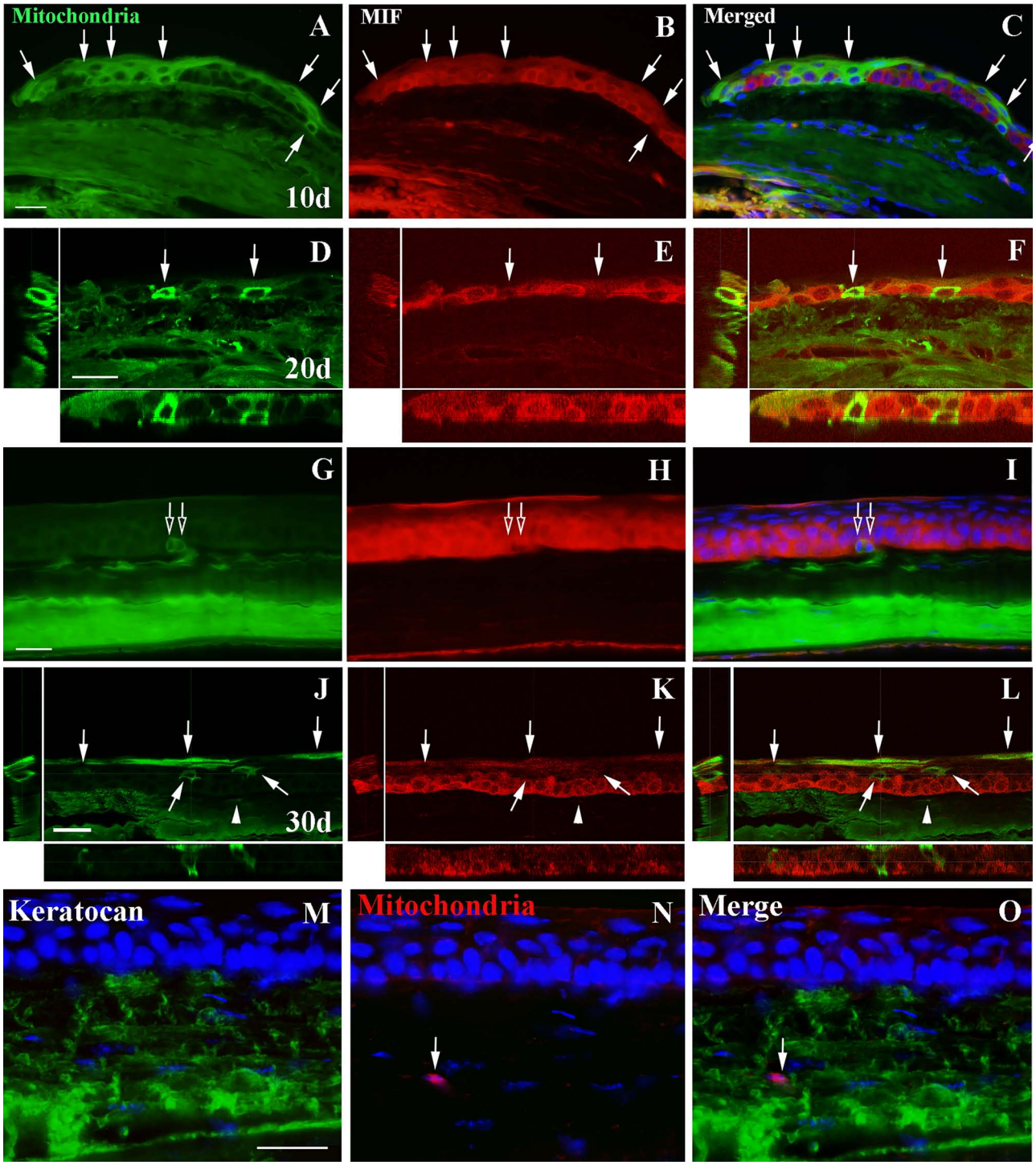

Figure 2. Analysis of the incorporation of mitochondria + hBMSCs in the mice cornea 10, 20, and 30 days postinjection. (A–C) Mitochondria^{+}/MIF^{-} cells (arrows) localized in the margin of the epithelium of conjunctiva (left) and cornea (right), 10 days postinjection. (D–I) Mitochondria^{+}/MIF^{-} cells localized in the margin of the epithelium (arrows in D, E, F) and in the basal strata of the central epithelium (empty arrows in G, H, I) 20 days postinjection. (J–L) Mitochondria^{+}/MIF^{-} cells (arrows) localized in the basal and in the superficial stratum of the central epithelium 30 days postinjection. Some mitochondria^{+}/MIF^{-} processes of keratocytes are located in the corneal stroma (arrowheads). Mitochondria^{+}/keratocan^{+} cells are located in the stroma (arrow) (M–O). The nuclei in (C), (F), (I), (L), (M), (N), and (O) are labeled with DAPI (blue). A longitudinal and transversal section of (D–F) and (J–L) is shown in each one. Scale bars: 20 μm (A–L); 25 μm (M–O).

(Fig. 3A–E). In the stroma, GFP$^+$ cells displayed a keratocyte-like morphology, lying between bundles of collagen fibrils (Fig. 3F, G). Finally, we also found GFP-labeled cells in the endothelium (Fig. 3H, I). After 40 days, the last stage was studied; the situation was similar to that of 30 days (data not shown).

Group II: hBMSC Injection in Mice With oGVHD

hBMSCs were injected, as previously described, into the right eye of BALB/c mice at day +15 after bone marrow transplantation, once the first signs of oGVHD were observed (Group II).

As early as 10 days after injection of the hBMSCs, the cornea showed significant changes in its structure, but as shown in Figure 4, a high number of GFP$^+$ cells were observed in several corneal levels. In detail, the corneal epithelium was atrophic and showed satellitosis, cell vacuolization, and the presence of apoptotic bodies (cells showing chromatin clumping and nuclear pyknosis in at least 8/10 biopsies analyzed). Notably, limbus epithelium showed the same histologic features than those observed in the corneal epithelium (27). Remarkably, the number of GFP$^+$ cells was higher than the previously observed at the same time point after hBMSCs subconjunctival injection in control mice (Group I).

Twenty days after injection, the left eye (noninjected) of all mice showed (in greater or lesser degree) loss of periocular fur, crusting of the eyelid margin, erythematous lids, and blepharospasm, whereas these features were not significantly observed in the right eye (injected) of the same animal (data not shown). The posterior histopathological examination of the cornea showed no signs of oGVHD in the right eye (Fig. 5A). By contrast, in the left eye, where hBMSCs had not been injected, examination revealed the presence of histological features of oGVHD such as atrophy, vacuolization, and apoptosis (Fig. 5B). No significant abnormalities were observed in the endothelial layer.

All mice receiving 5×10^6 BM cells and 5×10^6 donor splenocytes exhibited clinical features ≥1 of GVHD when sacrificed (25–35 days after the allogeneic transplantation): weight loss, hunched posture, poor skin integrity, abnormal fur texture, and decreased activity.

DISCUSSION

Several animal models and clinical trials have been designed to investigate the capability of MSCs to regenerate host tissues, but controversial information has been published about their migration, engraftment capacity, and function after in vivo injection. In this regard, BMSCs may improve the outcome after myocardial infarction not by regenerating cardiomyocytes but rather by secreting TNF-inducible gene-6, an anti-inflammatory protein that reduces infarct size and improves cardiac function (23). Furthermore, some studies describing the graft and differentiation of BMSCs into different host tissues have been criticized because a possible fusion between local tissue and infused cells cannot be ruled out.

In the current study, we show that GFP$^+$ hBMSCs are found in corneal tissue of BALB/c mice after subconjunctival injection. The mouse cornea differs from the human in at least two important properties. Mouse cornea is much thinner than human cornea and, as such, is more readily accessible to cell-based therapy. Additionally, the collagen in human corneas is extensively cross-linked, resulting in a tougher, more stable tissue, possibly less amenable to remodeling than that of the mouse (12). These anatomical differences between human and murine cornea could potentially make this therapeutic approach less feasible in humans. However, the physiopathology of the oGVHD is known to be very similar in both species, which would support the extrapolation of the results to the human cornea. Interestingly, after injection, hBMSCs displayed morphological characteristics of epithelial, stromal, and endothelial cells and appear at different layers and in morphologies varying from cubic to flattened, depending on their position within the epithelium. Furthermore, these cells also displayed ultrastructural properties, such as bundles of intermediate filaments, hemidesmosomes, and desmosomes with other cells that are GFP$^-$, thus confirming their differentiation into epithelial cells. Recent data suggest that fusion could be the predominant mechanism by which hBMSCs may acquire epithelial characteristics (14). In order to rule out a possible fusion between GFP$^+$ cells and local mice epithelial or endothelial cells, we confirmed that GPF$^+$ cells were MIF$^-$, which demonstrates the human origin of differentiated GFP$^+$ cells. These results represent a major finding, which confirms that hBMSCs may induce their therapeutic effect not just by a paracrine effect but also by differentiation and regeneration of damaged tissues in the host. In this regard, although no direct genotype was performed to further validate our assays, we show that immunohistochemical figures were not due to cell fusions but to a true differentiation process, which is in accordance with previous data suggesting that BMSCs exert their beneficial effect by differentiation, without cell fusion (40). Moreover, their therapeutic effect in oGVHD could also be attributed to their anti-inflammatory and immunomodulatory properties (39). The exact contribution of both regenerative effect and immunomodulatory properties of BMSCs within this model will require further studies.

From a translational point of view, the current study is of particular interest since it confirms the therapeutic use of BMSCs in pathologies in which their regenerative as well as their immunomodulatory properties might be of benefit, such as ocular surface diseases or immune-mediated disorders, including graft-versus-host

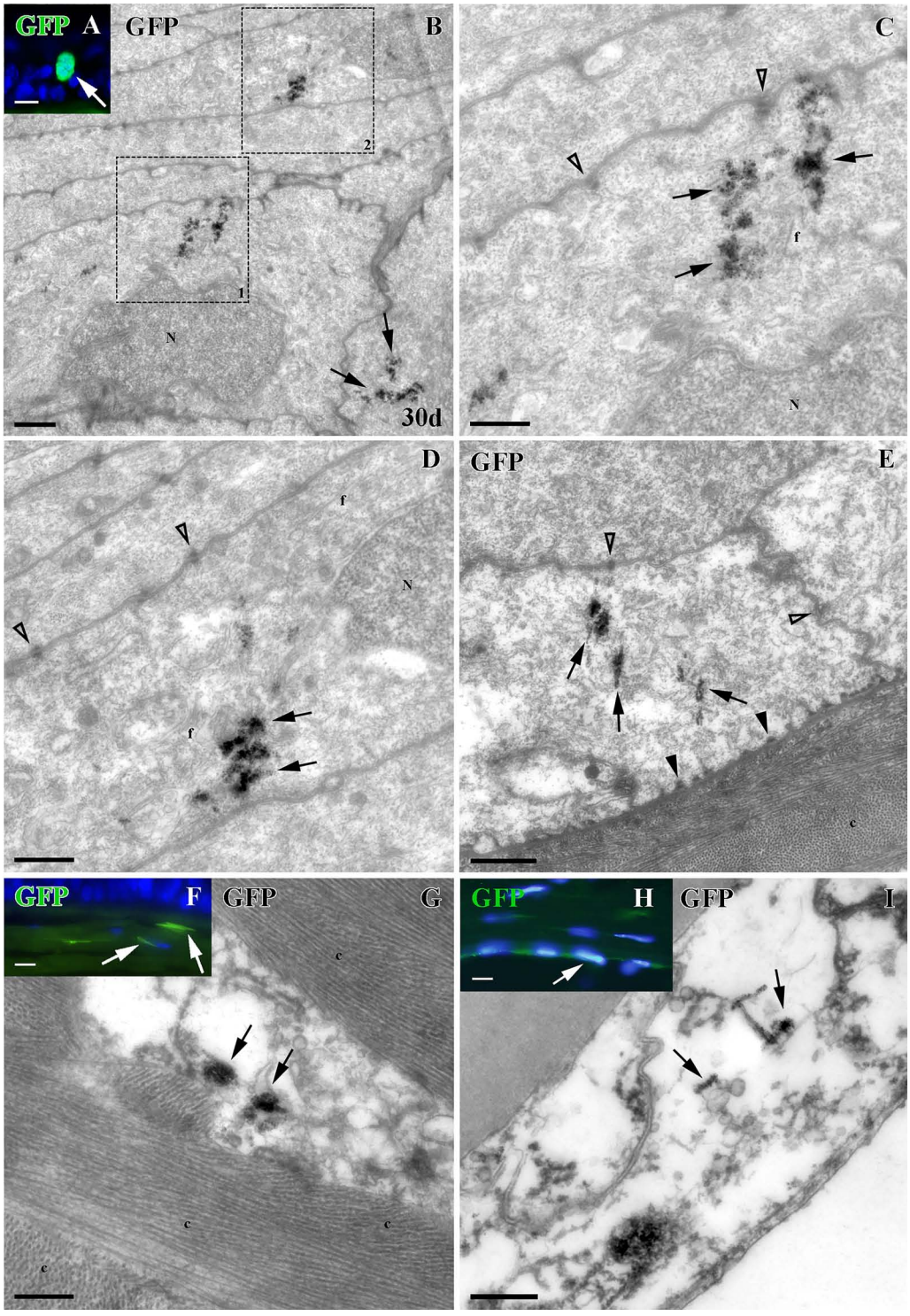

Figure 3. Immunofluorescence labeling and immunogold electron microscopy labeling (arrows) of GFP⁺ hBMSCs (green) in the mouse cornea 30 days postinjection. (A) GFP⁺ cells (arrow) in the epithelium. (B) GFP⁺ cells (arrow) in the epithelium. Squares 1 and 2 are enlarged in (C) and (D), respectively. (C) Detail of a GFP⁺ cell (arrows) with intermediate filaments (f) and desmosomes (empty arrowheads) in the lower strata of the epithelium. (D) Detail of a GFP⁺ cell (arrows) with intermediate filaments (f) and desmosomes (empty arrowheads) in the higher strata of the epithelium. (E) Detail of a basal GFP⁺ epithelial cell (arrows) showing desmosomes (empty arrowheads) and hemidesmosomes (arrowheads). (F) GFP⁺ keratocytes (arrows) in the stroma. (G) GFP⁺ keratocyte (arrows) surrounded by collagen packets (c) in the stroma. (H) GFP⁺ cells (arrow) in the endothelium. (I) GFP⁺ endothelial cells (arrows). The nuclei in (A), (F), and (L) are labeled with DAPI (blue). Scale bars: 10 μm (A, H, F); 1,000 nm (B, E); 500 nm (C–D, F–G, I). N, nucleus.

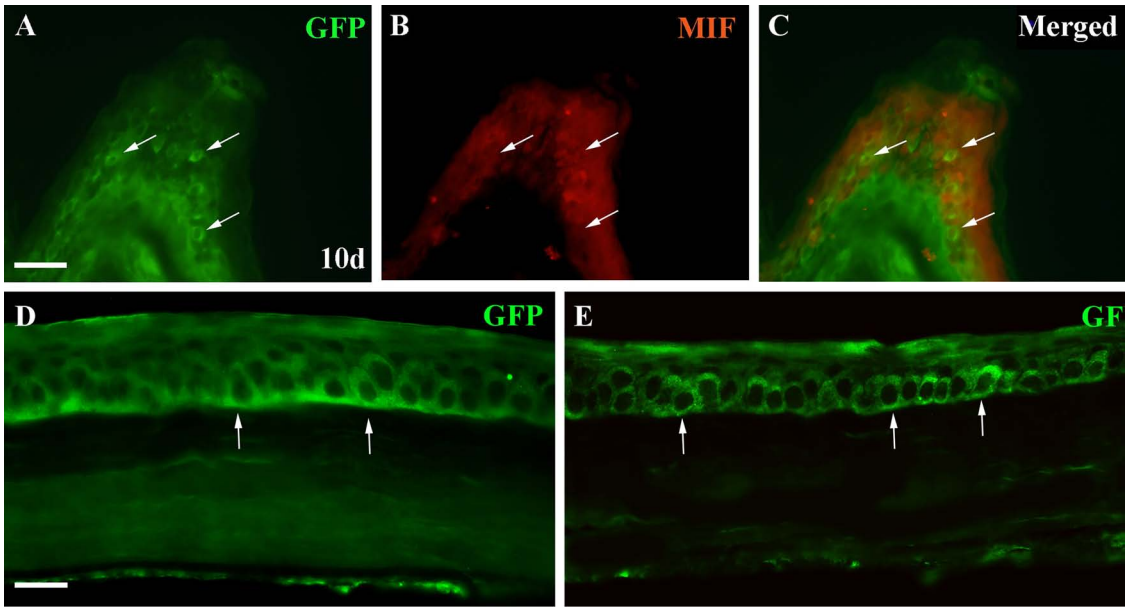

Figure 4. Distribution of GFP$^+$ hBMSCs in the corneal epithelium, stroma, and endothelium of the right eye of mice with oGVHD. Ten days after subconjunctival injection of hBMSCs. (A) GFP$^+$ cells (arrows); (B) MIF$^-$ cells; (C) GFP$^+$/MIF$^-$ cells (arrows). Twenty days after subconjunctival injection of hBMSCs (D, E), the corneal epithelium showed a massive infiltration with GFP$^+$/MIF$^-$ cells in all layers, from the basal to the superficial stratum of the central epithelium (arrows). Scale bars: 20 μm (A–E).

disease. In this regard, Oh et al. have described that BMSCs topically applied to damaged corneas display anti-inflammatory and antiangiogenic effects, which might contribute to their therapeutic effect after corneal wound healing, although the possible effect of BMSCs in the long term and their differentiation into the different corneal layer cells were not explored (29). Furthermore, topic instillation of BMSCs limits the availability of BMSCs and their potential to engraft in this study. Liu et al. have previously reported that umbilical MSCs and bone marrow MSCs can be directly injected into mouse corneal stroma and improve corneal transparency and stromal thickness in Lum$^{-/-}$ mice and Kera$^{-/-}$ mice (25,26). This effect was related to an improved organization of the collagen matrix and local differentiation into stromal cells. Also Du et al. directly injected human stromal stem cells into the corneal stroma of 8- to 10-week-old C57BL/6 mice and observed that human stem cells remained viable for long periods, secreted extracellular matrix components characteristic of human corneal stromal stem cells, did not evoke a CD3$^+$ T-cell response, and elicited only transitory inflammation (12). Interestingly, studies have recently reported that stromal cells can also be isolated and expanded from the limbus and may provide a supportive niche for epithelial stem cells (1,19,24). Furthermore, they possess immunosuppressive properties similar to MSCs obtained from other sources (15).

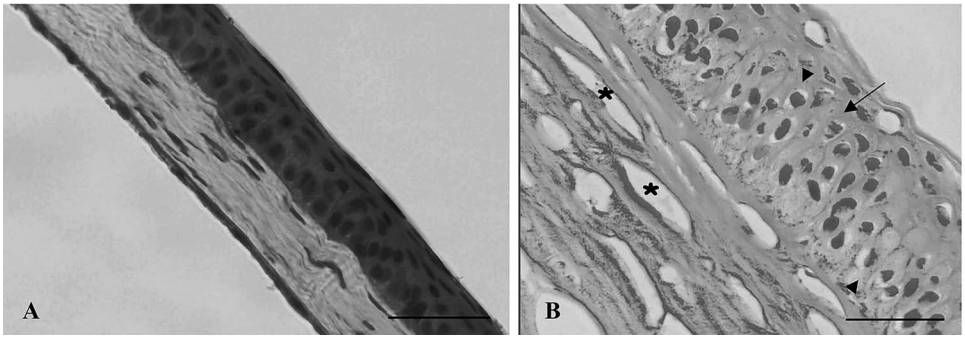

Figure 5. Images of corneal sections from mice with GVHD stained with hematoxylin and eosin. (A) Right eye treated with hBMSC injection showed no morphological signs of oGVHD; (B) left eye, untreated, showed cytoplasmic vacuolization (arrowheads) and apoptotic bodies (arrows) in the epithelium and stromal edema (asterisks). Scale bars: 50 μm.

In the current study, we were able to demonstrate not only stromal but also epithelial and endothelial differentiation of hBMSCs, not after local injection into the stromal cornea but after subconjunctival injection, thus providing evidence of the capability of hBMSCs to migrate into corneal layers and also describing an easy and less risky approach for the injection of hBMSCs not directly into the cornea but subconjunctivally. Furthermore, contrary to previous reports showing that hBMSCs do not engraft in the long term and remain detectable only for a few days after systemic injections long term, the current study demonstrates that the local injection could facilitate their local engraftment and differentiation (3).

Remarkably, oGVHD is a common complication after allogeneic transplantation and hampers the patient's quality of life. No therapeutic strategy has been described until now that favorably affects the outcome of oGVHD once it has been established. In fact, NIH indicates that ocular involvement might be considered irreversible, so that systemic immunosuppressive treatment should not be kept in these patients (32). The current study describes a new approach for the treatment of these patients, for which therapeutic interventions are rather limited. Furthermore, contrary to previous experiences using intravenous administration of hBMSCs in GVHD, the current study confirms that subconjunctival administration of these cells allows to induce both a durable engraftment and a local differentiation of hBMSCs, which contribute to avoid and/or repair the GVHD-induced tissue damage, as demonstrated by both macroscopic and histopathological finding in right (treated) versus left (untreated) eyes of mice undergoing transplantation.

In summary, the current study shows that hBMSCs are distributed across the whole mouse cornea after subconjunctival injection and acquire in vivo features characteristic of epithelium, stroma, and endothelium. Most importantly, we show that locally injected hBMSCs avoid GVHD-mediated corneal damage in an animal model.

ACKNOWLEDGMENTS: The authors would like to thank Didier Trono for pWPI vector plasmid. Teresa Caballero was supported by a Rio Hortega grant (code: CM10/00161) from Instituto de Salud Carlos III. We thank R. Sánchez and M. T. Sánchez for their technical assistance. We would like to thank Dr. Anton Martens, from the University Medical Center Utrecht, for providing the vectors for GFP assays. This study was partially supported by grants from FIS (PI11/02366 and PI12/00939) and Junta de Castilla y León (GR 183). The authors declare no conflicts of interest.

REFERENCES

1. Branch, M. J.; Hashmani, K.; Dhillon, P.; Jones, D. R.; Dua, H. S.; Hopkinson, A. Mesenchymal stem cells in the human corneal limbal stroma. Invest. Ophthalmol. Vis. Sci. 53:5109–5116; 2012.
2. Brissette-Storkus, C. S.; Reynolds, S. M.; Lepisto, A. J.; Hendricks, R. L. Identification of a novel macrophage population in the normal mouse corneal stroma. Invest. Ophthalmol. Vis. Sci. 43:2264–2271; 2002.
3. Caplan, A. I. Why are MSCs therapeutic? New data: New insights. J. Pathol. 217(2):318–324; 2009.
4. Carrancio, S.; Blanco, B.; Romo, C.; Muntión, S.; López-Holgado, N.; Blanco, J. F.; Briñon, J. G.; San Miguel, J. F.; Sánchez-Guijo, F. M.; del Cañizo, M. C. Bone marrow mesenchymal stem cells for improving hematopoietic function: An in vitro and in vivo model. Part 2: Effect on bone marrow microenvironment. PLoS One 6(10):e26241; 2011.
5. Carrancio, S.; López-Holgado, N.; Sánchez-Guijo, F. M.; Villarón, E.; Barbado, V.; Tabera, S.; Díez-Campelo, M.; Blanco, J.; San Miguel, J. F.; Del Cañizo, M. C. Optimization of mesenchymal stem cell expansion procedures by cell separation and culture conditions modification. Exp. Hematol. 36(8):1014–1021; 2008.
6. Cooke, K. R.; Kobzik, L.; Martin, T. R.; Brewer, J.; Delmonte, J. Jr.; Crawford, J. M.; Ferrara, J. L. An experimental model of idiopathic pneumonia syndrome after bone marrow transplantation: I. The roles of minor H antigens and endotoxin. Blood 88(8):3230–3239; 1996.
7. Cotsarelis, G.; Cheng, S. Z.; Dong, G.; Sun, T. T.; Lavker, R. M. Existence of slow cycling limbal epithelial basal cells that can be preferentially stimulated to proliferate: Implications on epithelial stem cells. Cell 57:201–209; 1989.
8. Chamberlain, G.; Fox, J.; Ashton, B.; Middleton, J. Concise review: Mesenchymal stem cells: Their phenotype, differentiation capacity, immunological features, and potential for homing. Stem Cells 25:2739–2749; 2007.
9. Chapel, A.; Bertho, J. M.; Bensidhoum, M.; Fouillard, L.; Young, R. G.; Frick, J.; Demarquay, C.; Cuvelier, F.; Mathieu, E.; Trompier, F.; Dudoignon, N.; Germain, C.; Mazurier, C.; Aigueperse, J.; Borneman, J.; Gorin, N. C.; Gourmelon, P.; Thierry, D. Mesenchymal tem cells home to injured tissues when co-infused with hematopoietic cells to treat a radiation-induced multi-organ failure syndrome. J. Gene Med. 5(12):1028–1038; 2003.
10. Devine, S. M.; Cobbs, C.; Jennings, M.; Bartholomew, A.; Hoffman, R. Mesenchymal stem cells distribute to a wide range of tissues following systemic infusion into nonhuman primates. Blood 101(8):2999–3001; 2003.
11. Dominici, M.; Le Blanc, K.; Mueller, I.; Slaper-Cortenbach, I.; Marini, F.; Krause, D.; Deans, R.; Keating, A.; Prockop, D. J.; Horwitz, E. Minimal criteria for defining multipotent mesenchymal stromal cells. The International Society for Cellular Therapy position statement. Cytotherapy 8(4):315–317; 2006.
12. Du, Y.; Carlson, E. C.; Funderburgh, M. L.; Birk, D. E.; Pearlman, E.; Guo, N.; Kao, W. W.; Funderburgh, J. L. Stem cell therapy restores transparency to defective murine corneas. Stem Cells 27(7):1635–1642; 2009.
13. Du, Y.; Funderburgh, M. L.; Mann, M. M.; SundarRaj, N.; Funderburgh, J. L. Multipotent stem cells in human corneal stroma. Stem Cells 23(9):1266–1275; 2005.
14. Ferrand, J.; Noël, D.; Lehours, P.; Prochazkova-Carlotti, M.; Chambonnier, L.; Ménard, A.; Mégraud, F.; Varon, C. Human bone marrow-derived stem cells acquire epithelial characteristics through fusion with gastrointestinal epithelial cells. PLoS One 6:e19569; 2011.
15. Garfias, Y.; Nieves-Hernández, J.; García-Mejía, M.; Estrada-Reyes, C.; Jiménez-Martínez, M. C. Stem cells isolated from the human stromal limbus possess immunosuppressant properties. Mol. Vis. 18:2087–2095; 2012.

16. Geuze, R. E.; Prins, H. J.; Öner, F. C.; van der Helm, Y. J.; Schuijff, L. S.; Martens, A. C.; Kruyt, M. C.; Alblas, J.; Dhert, W. J. Luciferase labeling for multipotent stromal cell tracking in spinal fusion versus ectopic bone tissue engineering in mice and rats. Tissue Eng. Part A 16:3343–3351; 2010.
17. Hamrah, P.; Liu, Y.; Zhang, Q.; Dana, M. R. The corneal stroma is endowed with a significant number of resident dendritic cells. Invest. Ophthalmol. Vis. Sci. 44:581–589; 2003.
18. Hamrah, P.; Zhang, Q.; Liu, Y.; Dana, M. R. Novel characterization of MHC class II-negative population of resident corneal Langerhans cell-type dendritic cells. Invest. Ophthalmol. Vis. Sci. 43:639–646; 2002.
19. Hashmani, K.; Branch, M. J.; Sidney, L. E.; Dhillon, P. S.; Verma, M.; McIntosh, O. W.; Hopkinson, A.; Dua, H. S. Characterization of corneal stromal stem cells with the potential for epithelial transdifferentiation. Stem Cell Res. Ther. 4(3):75; 2013.
20. Horwitz, E. M. Building bone from blood vessels. Nat. Med. 16:1373–1374; 2010.
21. Horwitz, E. M.; Dominici, M. How do mesenchymal stromal cells exert their therapeutic benefit? Cytotherapy 10(8):771–744; 2008.
22. Kawada, H.; Fujita, J.; Kinjo, K.; Matsuzaki, Y.; Tsuma, M.; Miyatake, H.; Muguruma, Y.; Tsuboi, K.; Itabashi, Y.; Ikeda, Y.; Ogawa, S.; Okano, H.; Hotta, T.; Ando, K.; Fukuda, K. Nonhematopoietic mesenchymal stem cells can be mobilized and differentiate into cardiomyocytes after myocardial infarction. Blood 104(12):3581–3587; 2004.
23. Lee, R. H.; Pulin, A. A.; Seo, M. J.; Kota, D. J.; Ylostalo, J.; Larson, B. L.; Semprun-Prieto, L.; Delafontaine, P.; Prockop, D. J. Intravenous hMSCs improve myocardial infarction in mice because cells embolized in lung are activated to secrete the anti-inflammatory protein TSG-6. Cell Stem Cell 5:54–63; 2009.
24. Li, G. G.; Zhu, Y. T.; Xie, H. T.; Chen, S. Y.; Tseng, S. C. Mesenchymal stem cells derived from human limbal niche cells. Invest. Ophthalmol. Vis. Sci. 53:5686–5697; 2012.
25. Liu, H.; Zhang, J.; Liu, C. Y.; Hayashi, Y.; Kao, W. W. Bone marrow mesenchymal stem cells can differentiate and assume corneal keratocyte phenotype. J. Cell. Mol. Med. 16(5):1114–1124; 2012.
26. Liu, H.; Zhang, J.; Liu, C. Y.; Wang, I. J.; Sieber, M.; Chang, J.; Jester, J. V; Kao, W. W. Cell Therapy of congenital corneal disease with umbilical cord mesenchymal stem cells: Lumican null mice. PLos One 19; 5(5):e10707; 2010.
27. Lorenzo-Pérez, R.; Pérez-Simón, J. A.; Caballero-Velázquez, T.; Flores, T.; Carrancio, S.; Herrero, C.; Blanco, B.; Gutierrez-Cosio, S.; Cañete-Campos, C.; Cruz-González, F.; San-Miguel, J. F.; Hernández-Galilea, E.; Sánchez-Abarca, I. Limbus damage in ocular graft-versus-host disease. Biol. Blood Marrow Transplant. 17(2):270–273; 2011.
28. Matsuda, A.; Tagawa, Y.; Matsuda, H.; Nishihira, J. Expression of macrophage migration inhibitory factor in corneal wound healing in rats. Invest. Ophthalmol. Vis. Sci. 38(8):1555–1562; 1997.
29. Oh, J. Y.; Kim, M. K.; Shin, M. S.; Lee, H. J.; Ko, J. H.; Wee, W. R.; Lee, J. H. The antiinflamatory and anti-angiogeneic role of mesenchymal stem cells in corneal wound healing following chemical injury. Stem Cells 26:1047–1055; 2008.
30. Oh, S. Y.; Choi, J. S.; Kim, E. J.; Chuck, R. S.; Park, C. Y. The role of macrophage migration inhibitory factor in ocular surface disease pathogenesis after chemical burn in the murine eye. Mol. Vis. 16:2402–2411; 2010.
31. Parrilla, M.; Lillo, C.; Herrero-Turrión, M. J.; Arévalo, R.; Lara, J. M.; Aijón, J.; Velasco, A. Pax2 in the optic nerve of the goldfish, a model of continuous growth. Brain Res. 1255:75–88; 2009.
32. Pavletic, S. Z.; Martin, P.; Lee, S. J.; Mitchell, S.; Jacobsohn, D.; Cowen, E. W.; Turner, M. L.; Akpek, G.; Gilman, A.; McDonald, G.; Schubert, M.; Berger, A.; Bross, P.; Chien, J. W.; Couriel, D.; Dunn, J. P.; Fall-Dickson, J.; Farrell, A.; Flowers, M. E.; Greinix, H.; Hirschfeld, S.; Gerber, L.; Kim, S.; Knobler, R.; Lachenbruch, P. A.; Miller, F. W.; Mittleman, B.; Papadopoulos, E.; Parsons, S. K.; Przepiorka, D.; Robinson, M.; Ward, M.; Reeve, B.; Rider, L. G.; Shulman, H.; Schultz, K. R.; Weisdorf, D.; Vogelsang, G. B.; Response Criteria Working Group. Measuring therapeutic response in chronic graft-versus-host disease: National Institutes of Health Consensus Development Project on Criteria for Clinical Trials in Chronic Graft-versus-Host Disease: IV. Response Criteria Working Group Report. Biol. Blood Marrow Transplant. 12:252–266; 2006.
33. Pérez-Simón, J. A.; López-Villar, O.; Andreu, E. J.; Rifón, J.; Muntión, S.; Campelo, M. D.; Sánchez-Guijo, F. M.; Martinez, C.; Valcarcel, D.; Cañizo, C. D. Mesenchymal stem cells expanded in vitro with human serum for the treatment of acute and chronic graft-versus-host disease: Results of a phase I/II clinical trial. Haematologica 96(7):1072–1076; 2011.
34. Pinnamaneni, N.; Funderburgh, J. L. Concise review: Stem cells in the corneal stroma. Stem Cells 30(6):1059–1063; 2012.
35. Schermer, A.; Galvin, S.; Sun, T. T. Differentiation-related expression of a major 64K corneal keratin in vivo and in culture suggests limbal location of corneal epithelial stem cells. J. Cell Biol. 103:49–62; 1986.
36. Shi, Y.; Hu, G.; Su, J.; Li, W.; Chen, Q.; Shou, P.; Xu, C.; Chen, X.; Huang, Y.; Zhu, Z.; Huang, X.; Han, X.; Xie, N.; Ren, G. Mesenchymal stem cells: A new strategy for immunosuppression and tissue repair. Cell Res. 20(5):510–518; 2010.
37. Tabera, S.; Pérez-Simón, J. A.; Díez-Campelo, M.; Sánchez-Abarca, L. I.; Blanco, B.; López, A.; Benito, A.; Ocio, E.; Sánchez-Guijo, F. M.; Cañizo, C.; San Miguel, J. F. The effect of mesenchymal stem cells on the viability, proliferation and differentiation of B-lymphocytes. Haematologica 93:1301–1309; 2008.
38. Usui, T.; Yamagami, S.; Kishimoto, S.; Seiich, Y.; Nakayama, T.; Amano, S. Role of macrophage migration inhibitory factor in corneal neovascularization. Invest. Ophthalmol. Vis. Sci. 48(8):3545–3550; 2007.
39. Wang, Y.; Chen, X.; Cao, W.; Shi, Y. Plasticity of mesenchymal stem cells in immunomodulation: Pathological and therapeutic implications. Nat. Immunol. 15(11):1009–1016; 2014.
40. Xu, H.; Miki, K.; Ishibashi, S.; Inoue, J.; Sun, L.; Endo, S.; Sekiya, I.; Muneta, T.; Inazawa, J.; Dezawa, M.; Mizusawa, H. Transplantation of neuronal cells induced from human mesenchymal stem cells improves neurological functions after stroke without cell fusion. J. Neurosci. Res. 88:3598–3609; 2010.